ORIGINAL ARTICLE

Impaired Visual Object Processing Across an Occipital-Frontal-Hippocampal Brain Network in Schizophrenia

An Integrated Neuroimaging Study

Pejman Sehatpour, MD, PhD; Elisa C. Dias, PhD; Pamela D. Butler, PhD; Nadine Revheim, PhD; David N. Guilfoyle, PhD; John J. Foxe, PhD; Daniel C. Javitt, MD, PhD

Context: Perceptual closure is the ability to identify objects based on partial information and depends on the function of a distributed network of brain regions that include the dorsal and the ventral visual streams, prefrontal cortex (PFC), and hippocampus.

Objective: To evaluate network-level interactions during perceptual closure in schizophrenia using parallel event-related potential (ERP), functional magnetic resonance imaging (fMRI), and neuropsychological assessment.

Design: Case-control study.

Setting: Inpatient and outpatient facilities associated with the Nathan Kline Institute for Psychiatric Research.

Patients: Twenty-seven patients with schizophrenia or schizoaffective disorder and 23 healthy controls.

Intervention: Event-related potentials were obtained from 24 patients and 20 healthy volunteers in response to fragmented (closeable) and control-scrambled (noncloseable) line drawings. Functional MRI was performed in 11 patients and 12 controls.

Main Outcome Measure: Patterns of between-group differences for predefined ERP components and fMRI regions of interest were determined using both analysis of variance and structural equation modeling. Global neuropsychological performance was assessed using standard neuropsychological batteries.

Results: Patients showed impaired generation of event-related components reflecting early sensory and later closure-related activity. In fMRI, patients showed impaired activation of the dorsal and ventral visual regions, PFC, and hippocampus. Impaired activation of dorsal stream visual regions contributed significantly to impaired PFC activation, which contributed significantly to impaired activation of the hippocampus and ventral visual stream. Impaired ventral stream and hippocampal activation contributed significantly to deficits on neuropsychological measures of perceptual organization.

Conclusions: Schizophrenia is associated with severe activation deficits across a distributed network of sensory and higher order cognitive regions. Deficit in early visual processing within the dorsal visual stream contributes significantly to impaired frontal activation, which, in turn, leads to dysregulation of the hippocampus and ventral visual stream. Dysfunction within this network underlies deficits in more traditional neurocognitive measures, supporting distributed models of brain dysfunction in schizophrenia.

Arch Gen Psychiatry. 2010;67(8):772-782

COGNITIVE DYSFUNCTION IS a critical component of schizophrenia and a major predictor of impaired long-term outcome.[1] Recent models of neurocognitive impairment focus on distributed dysfunction within widespread neuronal networks, with deficits in sensory processing along with higher-level impairment.[2] To date, however, the interrelationships between perceptual-level and higher-order components of neurocognitive impairment remain poorly understood. The present study uses multimodal event-related potential (ERP) and functional magnetic resonance imaging (fMRI) to assess distributed neural processing in schizophrenia within the context of a perceptual closure task, which is known to depend on interrelated bottom-up and top-down neural mechanisms.[3]

Perceptual closure refers to the ability of the brain to recognize an object even when presented with only fragmentary information (eg, a cat behind venetian blinds). Successful object recognition is indexed by generation of closure negativity (N_{CL}), peaking at approximately 240 milliseconds, which indexes activation of neuronal structures located within ventral

Author Affiliations are listed at the end of this article.

stream visual areas such as the lateral occipital complex (LOC).[4,5] Lateral occipital complex activation, in turn, depends on convergent bottom-up and top-down processes.[6-10] Prior studies have demonstrated significantly impaired LOC activation in schizophrenia along with impaired object recognition processes.[11]

The LOC receives convergent visual input from the magnocellular and parvocellular visual system. The magnocellular system is specialized for rapid conduction of low-resolution information to the dorsal visual stream, which plays a critical role in representation of spatial information and guiding attention and is thus commonly referred to as the "where" pathway. Dorsal stream projections to the prefrontal cortex (PFC) activate low-resolution image representations within this region,[12] which in turn provide top-down "framing" input to the hippocampal and LOC regions. In contrast, the parvocellular system provides slower, higher-resolution visual information that projects directly to the LOC.[13] Because of the more rapid transit of information through the magnocellular/dorsal stream pathway than through the parvocellular/ventral stream, information from the 2 pathways converges in LOC within the temporal window of object identification.

In ERP, magnocellular/dorsal stream activation is reflected in generation of visual P1 (approximately 100 milliseconds), which indexes bottom-up activation of structures such as cortical visual area V3A.[6] Subsequent activation is observed over the PFC[10,14] and in individuals with implanted intracranial electrodes in the hippocampus.[3] Generation of N_{CL} is preceded by a marked neurophysiological synchrony between the hippocampus and LOC, suggesting that magnocellular-driven top-down information flow through the PFC/hippocampal loop provides critical framing input to the ventral stream closure process.

Parvocellular/ventral stream activation is reflected in generation of the visual N1 (approximately 170 milliseconds) potential, which reflects initial parvocellular-driven input to the LOC. For simple objects that can be identified without top-down input such as illusory contour detection, closure processes are reflected by modulation of the N1 potential itself.[8] However, for more complex processes,[15] such as closure of fragmented images, the closure process is delayed,[5] reflecting the need for convergent bottom-up and top-down processes.[16] Activation of brain regions involved in the perceptual closure process are reflected as well in differential activation of the dorsal/ventral visual regions, PFC, and hippocampus to nonfragmented vs fragmented images, with the high spatial resolution of MRI complementing the high temporal resolution of ERP.

Prior schizophrenia studies have demonstrated impaired N_{CL} generation using ERP along with behavioral closure impairments.[11] Parallel studies, in turn, have demonstrated impaired early magnocellular/dorsal stream processing,[17] suggesting potential loss of bottom-up input to PFC and hippocampal nodes of the perceptual closure network. However, assessment of the hippocampal node of this network, in particular, requires convergent fMRI/ERP assessment, as hippocampal generated activity is poorly represented in scalp ERP. The present study is the first to use a combined ERP/fMRI approach to assess network dysfunction underlying impaired perceptual closure processing in schizophrenia.

Finally, the present study evaluates the relationship between ERP/fMRI activation to perceptual closure stimuli and impairments in perception-related neuropsychological tasks. In particular, the Wechsler Adult Intelligence Scale III (WAIS-III) includes the picture arrangement test as well as subtests, including the Perceptual Organization Index, a component of the performance IQ index.[18] Similarly, the Measurement and Treatment Research to Improve Cognition in Schizophrenia (MATRICS) battery[2] incorporates the Brief Visual Memory Task, which assesses visual/perceptual processing. Although performance deficits on these measures are well established in schizophrenia, the underlying brain substrates are poorly understood.

Overall, in this study, we hypothesized that (1) patients would show deficits in fMRI as well as ERP indices of dorsal stream activation and closure, (2) deficits in dorsal stream activation would predict dysfunction throughout the closure circuit, and (3) closure deficits would be correlated with impairment in performance IQ related to assessment of perceptual organization.

METHODS

PARTICIPANTS

Data were collected in 2 separate experiments. In experiment 1 (ERP), 24 male patients who met *DSM-IV* criteria for schizophrenia (n=22) or schizoaffective disorder (n=2) and 20 healthy volunteers (17 male) of similar age participated. In experiment 2 (fMRI), 11 patients (10 male) who met criteria for schizophrenia (n=9) or schizoaffective disorder (n=2) and 12 healthy volunteers (11 male) of similar age participated. Eight male patients and 9 controls (8 male) participated in both experiments, so that the total sample included 27 patients (26 male, 1 female) and 23 controls (20 male, 3 female). Experiment 1 consisted of a single ERP session and experiment 2 was part of a larger fMRI study.

Patients were recruited from inpatient and outpatient facilities associated with the Nathan Kline Institute for Psychiatric Research. Diagnoses were obtained using the Structured Clinical Interview for *DSM-IV*.[19] Healthy volunteers with a history of Structured Clinical Interview for *DSM-IV*–defined Axis I psychiatric disorder were excluded. Subjects were excluded if they had any neurological or ophthalmologic disorders that might affect performance or if they met criteria for alcohol or substance dependence within the last 6 months or abuse within the last month. Informed consent was obtained after full explanation of procedures.

Patient and control groups did not differ significantly in age (mean [SD]: patients, 38.9 [10.5] years; controls, 33.3 [10.0] years). Brief Psychiatric Rating Scale[20] mean total score was 37.4 (SD, 9.4; n=26) and the Scale for the Assessment of Negative Symptoms[21] mean total score (including global scores) was 34.0 (SD, 16.0; n=26). All patients were receiving antipsychotics, with 20 patients receiving atypical antipsychotics, 3 patients receiving typical antipsychotics, and 4 patients receiving a combination of atypical and typical antipsychotics. The mean chlorpromazine equivalent was 1225 mg/d (SD, 589.5 mg/d). Mean duration of illness was 18.1 years (SD, 9.9 years).

STIMULI AND TASK

Methods were described previously for ERP and fMRI studies.[3,10] Briefly, fragmented line drawings of natural and man-made objects were drawn from the normed Snodgrass and Vanderwart picture set,[22,23] as shown in **Figure 1**. For ERP, stimuli were

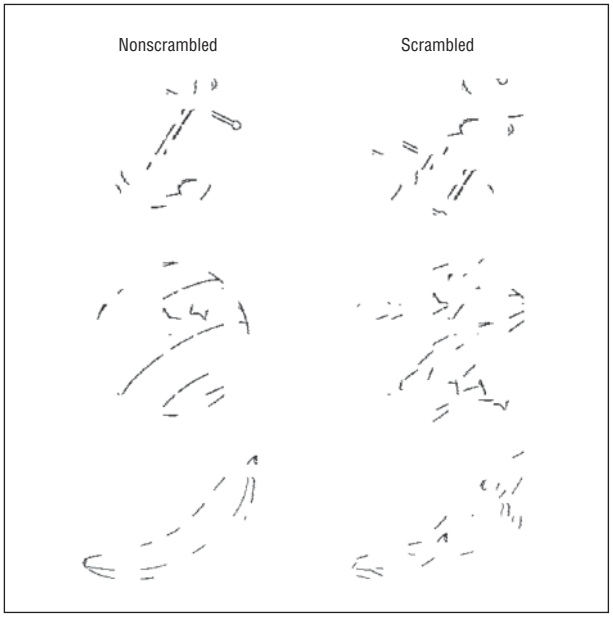

Figure 1. Examples of stimuli. Line drawings were taken from the Snodgrass and Vanderwart picture set.[22,23] From these images, segments containing black pixels were randomly and cumulatively deleted to produce 7 incrementally fragmented versions of each picture.[24] For this study, only images belonging to the third level of fragmentation were used; they are associated with 73% correct performance in normal individuals.[5] Fragmented stimuli were presented either in original nonscrambled form or were additionally scrambled to prevent object identification.[10] The images from top to bottom are an anchor, ball, and banana.

presented on an Iiyama Vision Master Pro 502 monitor located 143 cm from the subject. Images subtended a mean 4.8° (SD, 1.4°) and 4.4° (SD, 1.2°) of angle in the vertical and horizontal planes, respectively. For fMRI, stimuli were delivered through magnetic resonance–compatible liquid crystal display goggles.

TIMING OF STIMULUS PRESENTATION FOR THE ERP STUDY

For ERP, each image appeared for 750 milliseconds, followed by a blank screen (800 milliseconds), a "Y/N" prompt (200 milliseconds) requesting subjects to indicate by button press whether the object was recognizable vs scrambled, and a second blank screen (2200 milliseconds) showing the response window. If subjects pressed "Y" they were then requested to name the object. Only correctly named objects were considered correct "Y" responses. A total of 400 unique images (200 each, nonscrambled and scrambled) were presented in 8 runs (3.25 minutes/run).

TIMING OF STIMULUS PRESENTATION FOR THE fMRI STUDY

For fMRI, each image appeared for 500 milliseconds, followed by a 500-millisecond blank screen, resulting in a stimulus onset asynchrony of 1 second. Nonscrambled, scrambled, and complete (not used in present analyses) stimuli were presented in a block design. Each block consisted of 24 unique, nonrepeated images. Twelve blocks total (4 blocks × 3 stimulus types) were presented per subject. Order of stimuli was pseudorandomly distributed across subjects but organized such that the complete version of a stimulus was never presented prior to either the scrambled and incomplete versions. To ensure central fixation, subjects were asked to respond by button press whenever an irrelevant image (a dog, 4.2% probability) was presented.

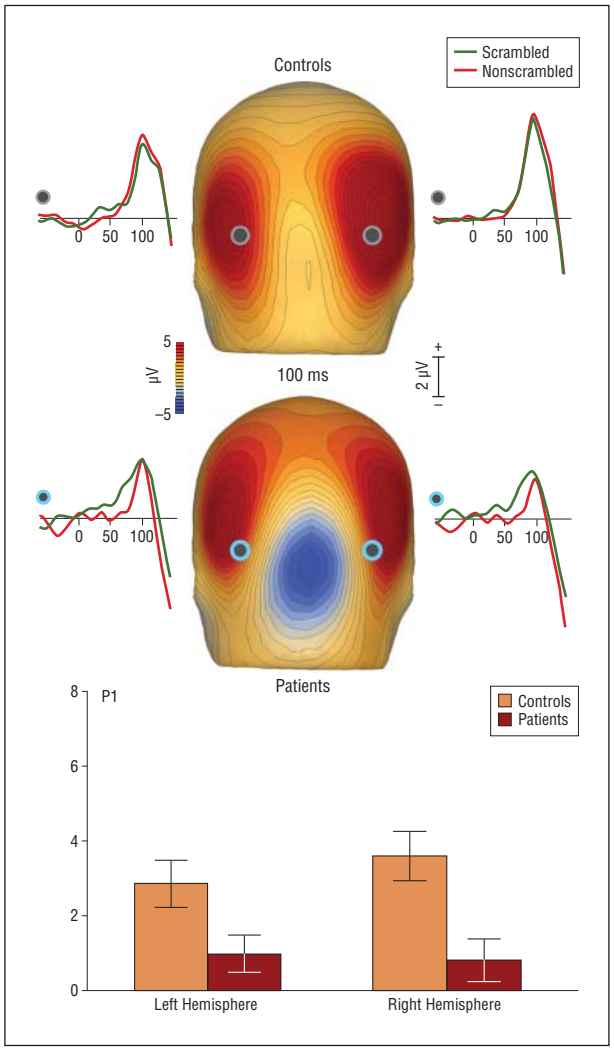

Figure 2. Event-related potential responses to the nonscrambled and scrambled stimuli over the posterior scalp and scalp voltage maps of the response to the nonscrambled stimuli. Voltage maps at 100 milliseconds show the observed positivity (P1) in controls and in patients. The graphs show scalp recordings from 2 representative occipital electrodes (PO5/PO6) in controls and patients, indicating no significant differences between the conditions in either group. The bar graph shows significant differences between the groups in the amplitude of responses to the nonscrambled stimuli.

ELECTROENCEPHALOGRAPHY DATA ACQUISITION AND ANALYSIS

Continuous electroencephalography was acquired using a BioSemi ActiveTwo electrode system with 168 scalp electrodes that was digitized at 512 Hz and re-referenced to the nose. Data were analyzed using BESA, version 5.1 (Brain Electric Source Analysis, MEGIS Software GmbH). Electrode channels were subjected to an artifact criterion of ±120 μV from –100 to 500 milliseconds. The vertical and horizontal electrooculograms were, in addition, visually inspected for blinks and large eye movements. For each subject, epochs were calculated for a time window from –100 to 500 milliseconds poststimulus and baseline-corrected relative to the prestimulus baseline. Accepted trials were then averaged separately for both nonscrambled and scrambled stimulus conditions to compute the visual evoked potential. Only identified stimuli were included in averages for nonscrambled stimuli. A priori analysis[10,11] tested between-group differences in amplitude of the ERP components P1, N1, N_{CL}, and frontal closure-related activity (N^{f}_{CL}) within predetermined spatial and temporal windows (information in legends to **Figure 2** and **Figure 3**).

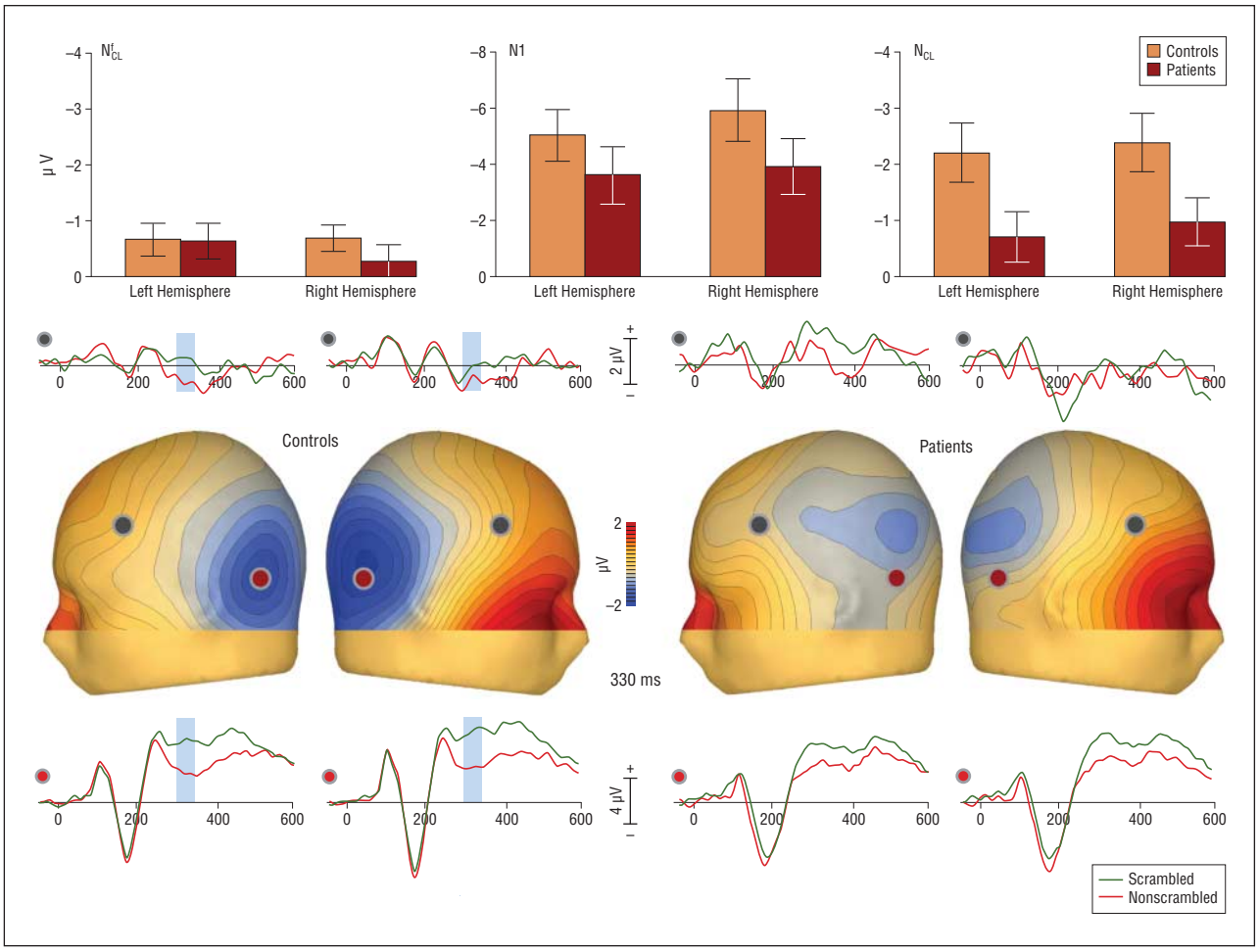

Figure 3. Voltage maps at 330 milliseconds (peak N_{CL} activity) illustrate the relative negativity over lateral occipital scalp for nonscrambled vs scrambled stimuli. The graphs show scalp recordings from 2 representative lateral occipital electrodes (PO7/PO8) and 2 representative lateral frontal electrodes (FC5/FC6) in controls and patients. The blue ribbon in the graphs show the tested window of time when the responses to the nonscrambled stimulus condition (in red) produced significantly larger negativity when compared with the scrambled pictures (in green). The bar graphs show significant differences between the groups in the amplitude of responses to the nonscrambled vs scrambled stimuli at the lateral occipital (N_{CL}) but not at the frontal scalp (N^f_{CL}). The graphs do not show any significant differences between the groups in the amplitude of responses for N1.

fMRI DATA ACQUISITION AND ANALYSIS

Images were acquired at the Center for Advanced Brain Imaging at the Nathan Kline Institute on a 3-T MRRS (formerly SMIS, Guildford, England) MRI system. This system uses a 38-cm inner diameter gradient coil with a gradient strength of 40 mT/m, rise time of 280 microseconds, and a 30-cm inner diameter transmission line radio frequency coil (Morris Instruments). In each run, T2*-weighed echoplanar functional images (repetition time = 2000 milliseconds, flip angle = 90°, matrix size = 64 × 64, field of view = 224 mm, voxel size = 3.5 mm^3) that emphasized the blood oxygenation level–dependent response were acquired while the participant attended to the visual stimuli. High-resolution (1 mm^3), T1-weighed anatomical images of the whole brain were acquired from each subject using a standard 3-dimensional magnetization-prepared rapid gradient echo pulse sequence to allow volume statistical analyses of signal changes. Head movement was minimized with the use of a custom-made head holder. In all subjects, motion never exceeded 0.75 mm along any axis.

The BrainVoyager QX software package[25] was used to process the fMRI data. Each subject's data were analyzed separately. Preprocessing of functional scans included slice scan time correction, head movement measurements, removal of linear trends, and temporal high-pass filtering. Each subject's functional data were coregistered with the anatomical data. The functional data were then transformed into Talairach space[26] for the multisubject analysis. Group statistical maps were obtained using a random-effect analysis of the blood oxygenation level–dependent signal time series. To estimate the blood oxygenation level–dependent response associated with each condition, regressors representing the timing of each of the stimulation epochs were convolved with a canonical function adjusted with a double-gamma hemodynamic response delay[27] and used in a multiple regression analysis. The resulting statistical maps were then grouped to obtain activation maps (**Figure 4** and **Figure 5**). The *P* values of the statistical maps were corrected for multiple comparisons[28,29] and *z*-normalized. Different conditions were then contrasted using a general linear model.[30,31]

Based on an a priori hypothesis, the coordinates from the intracranial generators of the P1, N_{CL}, N^f_{CL},[10] and hippocampus[3] were used to define regions of interest (ROIs) centered around these coordinates with a spread range of 10 mm^3. These resulted in an ROI at the dorsal visual stream, LOC, PFC, and hippocampal formation, respectively, from which the parameter estimates (β values) were derived and subjected to a multivariate analysis of variance.

CLINICAL VARIABLES

In addition to ERP and fMRI, several relevant neuropsychological measures were administered. These included the WAIS-

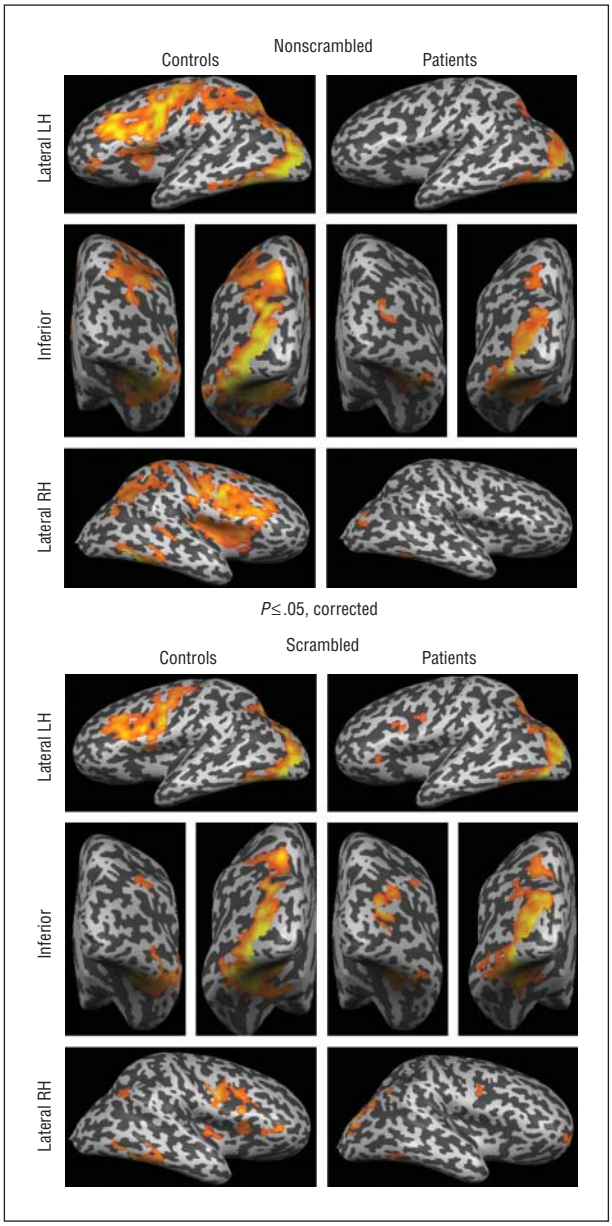

Figure 4. Functional magnetic resonance imaging group activation maps for controls and patients in response to the nonscrambled and scrambled conditions. The functional data are presented on the Talairach-normalized inflated brain of a single subject. All data are $P \leq .05$, corrected for multiple comparisons across the entire image volume. Areas of significant blood oxygenation level–dependent signal in the visual stream and prefrontal cortical regions are observed. LH indicates left hemisphere; RH, right hemisphere.

III picture arrangement test[18]; the Perceptual Organization Index battery, which consists of picture completion, matrix reasoning, and block design tests and the Processing Speed Index from the WAIS-III; the Working Memory Index (WMI) from the Wechsler Memory Scale III[32]; and the Brief Visuospatial Memory Test (BVMT-R),[33] which assesses retention of visual memory over time.

STATISTICAL ANALYSIS

Between-group analyses for ERP and fMRI measures were performed using a separate repeated-measures multivariate analysis of variance for each identified ERP component (P1, N1, N_{CL}, and N^{f}_{CL}) and for each of the 4 ROIs in fMRI studies (dorsal stream, LOC, PFC, and hippocampus). Analyses were conducted using SPSS software (SPSS Inc, Chicago, Illinois), with a between-subjects factor of group (patients and controls) and within-subjects factors of condition (nonscrambled and scrambled) and hemisphere. All tests were 2-tailed with a preset α level of $P < .05$.

Interrelationship among measures was determined by linear regression, supplemented with structural equation modeling (path analysis). Path analysis was implemented using AMOS 7.0 (SPSS Inc).[34] Selection among alternative models was determined by minimizing χ^2 variance, with paths entered according to the criterion χ^2 to include = $(\chi^2_{without} - \chi^2_{with})$, $(df_{without} - df_{with})$. Residual error and goodness of fit measures, including minimum sample discrepancy/*df*, root mean square error of approximation, and normed fit index, were used to assess model integrity. All significance levels are 2-tailed with a preset α level for significance of $P < .05$. Values in the text are mean (SD) unless otherwise specified.

RESULTS

BEHAVIORAL RESULTS

Patients recognized the nonscrambled objects 50.6% of the time vs 67.5% for controls ($t_{42} = -3.7$, $P = .002$). However, both groups scored substantially above chance, which was essentially 0, as the task consisted of naming the object with no information other than the fragmented image. The groups did not differ in their reaction times (patients, 1647 milliseconds [503 milliseconds]; controls, 1870 milliseconds [388 milliseconds]; $t_{42} = -1.6$, $P = .1$). Control values are similar to those obtained previously.[10]

ELECTROPHYSIOLOGICAL RESULTS

The ERP measures were assessed at predefined electrodes within predefined intervals based on prior studies with these stimuli in normal volunteers.[10] Separate analyses were conducted for the sensory components P1 and N1 and for closure-related components over LOC (N_{CL}) and PFC (N^{f}_{CL}).

SENSORY POTENTIALS

P1 was maximal over dorsal stream electrodes (PO5/PO6) within the 90- to 110-millisecond interval (Figure 2). P1 amplitudes were significantly reduced in patients relative to controls ($F_{1,42} = 7.0$, $P = .008$). The group × hemisphere ($F_{1,42} = 4.3$, $P = .045$) interaction was also significant, reflecting differential asymmetry between groups. Group × condition ($F_{1,42} = 1.3$, $P = .3$) and group × condition × hemisphere ($F_{1,42} = 0.02$, $P = .9$) interactions were not significant, reflecting similar P1 amplitude to nonscrambled and scrambled stimuli.

N1 was maximal over ventral stream electrodes (PO7/PO8) during the 160- to 180-millisecond latency range. N1 amplitude (Figure 3) was not significantly different between groups ($F_{1,42} = 1.8$, $P = .19$). Group × hemisphere ($F_{1,42} = 0.96$, $P = .33$), group × condition ($F_{1,42} = 0.05$, $P = .82$), and group × condition × hemisphere ($F_{1,42} = 0.62$, $P = .44$) interactions were also nonsignificant.

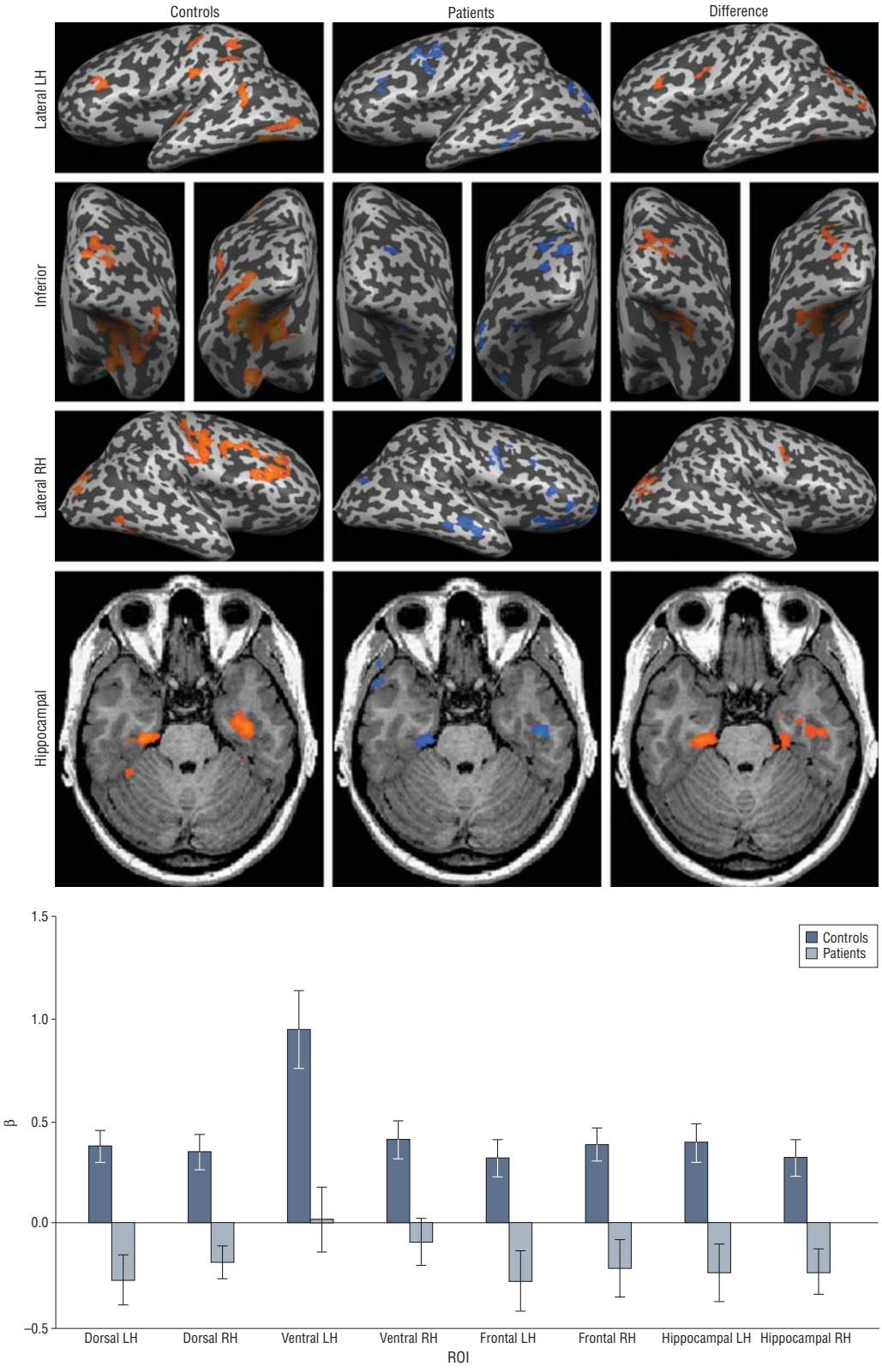

Figure 5. Functional magnetic resonance imaging responses for the nonscrambled vs scrambled comparison in controls, patients, and the difference between the 2 groups. In the functional magnetic resonance imaging activation maps for each group, red indicates a positive (nonscrambled > scrambled) and blue indicates a negative (nonscrambled < scrambled) direction in the blood oxygenation level–dependent (BOLD) signal change. Thus, the maps of the difference between the 2 groups illustrate areas of significant BOLD signal increase in controls compared with patients. The bar graph shows the magnitude of the BOLD signal change in response to the nonscrambled vs scrambled stimuli in controls and in patients at each region of interest (ROI), namely, the dorsal visual stream, ventral visual stream, lateral frontal cortex, and hippocampal formation. Significant differences between controls and patients are observed at the 4 ROIs bilaterally. Error bars indicate standard error of the mean; LH, left hemisphere; RH, right hemisphere.

Table 1. Analysis of Variance Showing Main Effect of Group and Group × Condition Interactions

ROI	Talairach Coordinate, x, y, z	Group		Group × Condition	
		$F_{1,21}$	*P* Value	$F_{1,21}$	*P* Value
Dorsal stream	±26, –79, 23	0.007	.93	27.04[a]	<.001
Ventral stream, LOC	±27, –59, – 8	1.782	.2	14.97[a]	.001
Frontal cortex	±33, 4, 40	5.5[a]	.03	14.26[a]	.001
Hippocampus	±24, –22, –23	0.442	.51	18.53[a]	<.001

Abbreviations: LOC, lateral occipital complex; ROI, region of interest; ±, symmetric Talairach positions.
[a] $P<.05$.

Table 2. Cortical Areas Outside the Predefined ROIs Where Significant Differential Activation to Stimuli Were Observed

Cortical Area	Talairach Coordinate[a]		
	x	y	z
Controls			
Right superior temporal	50	–48	17
Right inferior frontal	51	23	–10
Right middle frontal	38	58	–13
Left superior temporal	–50	12	–6
Left superior temporal	–62	–41	7
Left frontal precentral	–36	3	22
Left middle frontal	–42	44	22
Left parietal-angular	–32	–59	34
Left parietal-post central	–48	–23	41
Left globus pallidus	–19	–3	0
Left caudate	–21	8	20
Patients			
Right superior temporal	52	21	–18
Right middle temporal	58	–11	–10
Right frontal precentral	51	2.3	32
Right superior frontal	22	48	–1
Right inferior frontal	49	33	12
Right inferior frontal	24	26	–8
Left superior temporal	–54	13	0
Left temporal	–46	–17	–22
Left middle frontal	–33	41	–10
Left frontal precentral	–40	3	36

Abbreviation: ROI, region of interest.
[a] Talairach coordinates correspond to site of maximum statistical significance.

CLOSURE-RELATED POTENTIALS

Closure-related activity was observed primarily over the LOC, with a smaller contribution over frontal regions (Figures 3). As in prior studies, the N_{CL} was defined as the mean amplitude within a 300- to 330-millisecond latency range over left and right ventral stream electrodes (PO7/PO8). The expected significant main effect of condition was observed ($F_{1,42}=22.4$, $P<.001$), indicating differential activity across groups to nonscrambled vs scrambled stimuli. A significant group × condition was also found ($F_{1,42}=4.8$, $P=.04$), indicating reduced differential activity to nonscrambled vs scrambled in patients ($F_{1,23}=3.9$, $P=.06$) vs controls ($F_{1,19}=20.0$, $P<.001$). No significant main or interaction effects involving hemisphere were observed. Group × hemisphere ($F_{1,42}=0.15$, $P=.7$), condition × hemisphere ($F_{1,42}=0.94$, $P=.3$), and group × condition × hemisphere ($F_{1,42}=1.18$, $P=.3$) interactions involving LOC were not significant.

Bilateral differential activity was also observed over lateral-frontal scalp regions (FC5/FC6) within the N_{CL} time frame ($F_{1,42}=9.08$, $P=.004$). The group × condition interaction was not significant ($F_{1,42}=0.345$, $P=.56$).

fMRI RESULTS

Both experimental conditions (nonscrambled and scrambled) activated widespread and substantially overlapping cortical networks (Figure 4). Blood oxygenation level–dependent activation patterns were assessed within predefined ROIs based on prior studies with these stimuli in normal volunteers.[10] We investigated 4 brain regions—the dorsal visual stream, ventral visual stream, lateral PFC, and hippocampal formation—using multivariate analysis of variance, which revealed significant main effects of region ($F_{3,19}=7.9$, $P=.001$) and hemisphere ($F_{1,21}=11.8$, $P=.003$). No significant main effect of group was observed ($F_{1,21}=2.23$, $P=.15$), indicating absence of significant differences in the general activation of these brain regions across the 2 groups. However, significant effects for group × condition ($F_{1,21}=37.4$, $P<.001$), group × hemisphere ($F_{1,21}=5$, $P=.03$), and region × hemisphere ($F_{3,19}=4.5$, $P=.02$) were observed. No other significant interactions were found. Following a main effect of region, a set of preplanned analyses of variance were carried out to unpack the results observed at each region. Significant group × condition interactions were observed at all 4 regions bilaterally, indicating reduced closure-related activity in patients relative to controls (**Table 1**, **Table 2**, and Figure 5).

CORRELATION WITHIN ERP AND fMRI MEASURES

To determine contributions of early stage measures to subsequent closure-related activity, separate sets of analyses were conducted for ERP and fMRI data. For ERP data, correlational analyses using the differential activity to nonscrambled vs scrambled stimuli were used. However, because the hippocampal node was not represented in scalp-related activity, formal path analysis was not used. For fMRI data, a path analysis explored the interrelationship between ROIs, as well as the effect of cohort on pattern of interrelationships. Because only 8 subjects participated in both ERP and fMRI studies, correlation across modalities was not possible.

Event-Related Potentials

For both patients and controls, P1 amplitude correlated significantly with amplitude of N^f_{CL} (patients, $r=0.64$, $P=.001$; controls, $r=0.55$, $P=.01$). Also, in both groups, strength of N^f_{CL} correlated significantly with amplitude of N_{CL} (patients, $r=0.75$, $P<.001$; controls, $r=0.76$, $P<.001$). For patients ($r=0.64$, $P=.001$), but not controls ($r=0.28$, $P=.24$), deficits in P1 generation correlated significantly with deficits in N_{CL} generation over LOC.

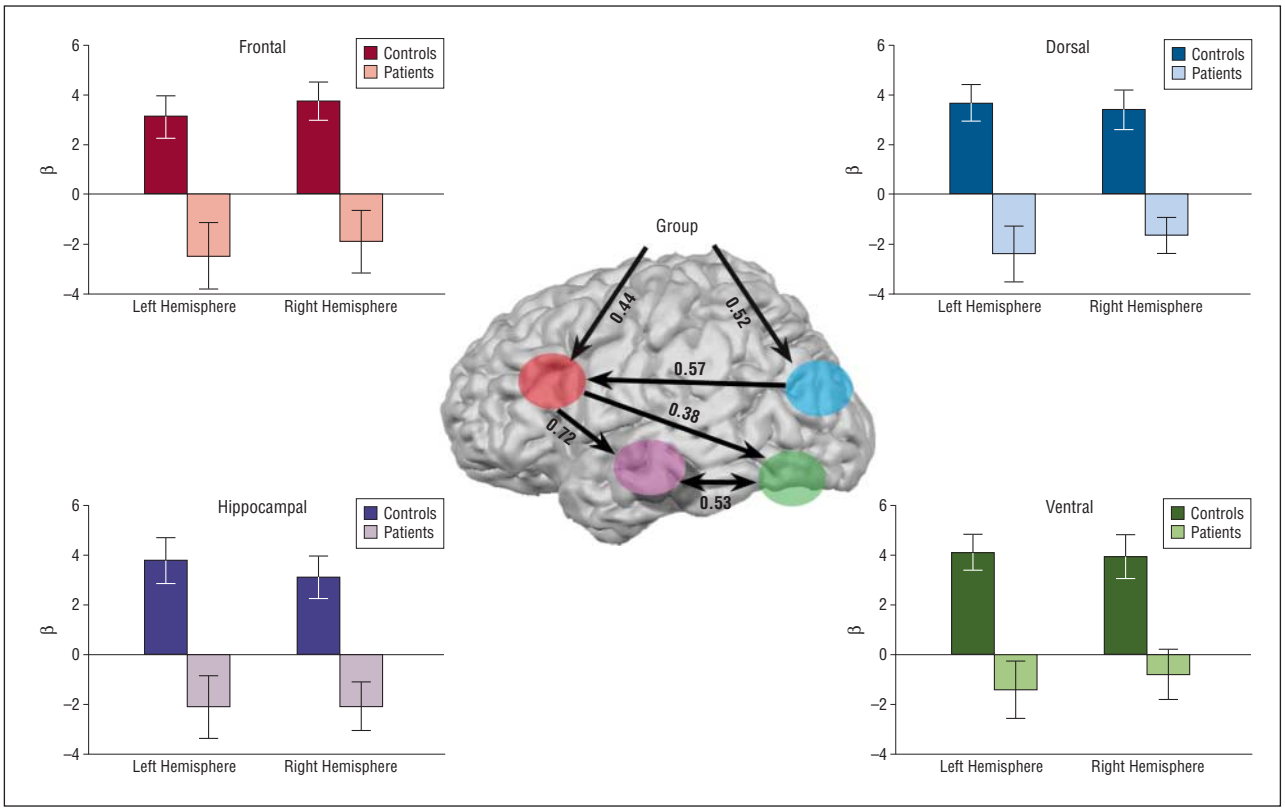

Figure 6. Path analysis of brain network interactions associated with impaired perceptual closure in schizophrenia. Differential activation indicated brain regions to closeable (nonscrambled) vs noncloseable (scrambled) images. Standard regression coefficients between regions are determined by path analysis based on iterative path fitting (all $P<.05$). Functional magnetic resonance imaging activations at dorsal stream and frontal regions significantly predicted group affiliation. Goodness of fit measures vs suggested rule of thumb values[34] for the model are as follows: minimum sample discrepancy=1.036 (rule of thumb <2.0), normed fit index, 0.949 (rule of thumb >0.9); root mean square error of approximation, 0.027 (rule of thumb <0.05); and Hoelter 0.05=113.

Functional MRI

Interrelationship among regions was assessed using path analysis. An iterative model was used, with paths added to the model only to the extent that they statistically reduced free variance. Significant paths were observed from the dorsal visual stream to PFC, PFC to LOC, and PFC to hippocampal formation. In addition, a bidirectional interaction was observed between hippocampal formation and the ventral visual stream (**Figure 6**). When group was entered into the model, significant independent effects of diagnosis were observed on dorsal stream and frontal nodes, but not with hippocampal formation or ventral visual stream, suggesting significant effects of pathological processing primarily on processing within dorsal stream and frontal regions.

CORRELATION BETWEEN ERP/fMRI AND CLINICAL MEASURES

Mean performance IQ in patients with schizophrenia was 86.7 (17.3), which is significantly lower than the normative mean of 100 ($t_{22}=3.68$, $P=.001$). Patients showed significant reductions in picture arrangement ($t=2.25$, $P=.03$), Perceptual Organization Index ($t=2.62$, $P=.02$), Processing Speed Index ($t=10.8$, $P=.001$), and WMI scores ($t=3.46$, $P=.002$) relative to published norms, with greater deficit on the Processing Speed Index relative to the Perceptual Organization Index ($t=3.31$, $P=.003$) (**Table 3**).

Deficits in fMRI activation of the LOC correlated significantly with picture arrangement scores as well as the overall Perceptual Organization Index and matrix reasoning subtest. In contrast, no significant correlation was observed between LOC activity and Processing Speed Index, WMI, or BVMT-R scores (Table 3). Significant correlations were also observed between hippocampal activation and several indices of visual processing as well as with BVMT-R score. No significant correlations were observed between frontal or dorsal ROI activations and indices of perceptual closure (all, $P>.2$). Similar correlations were observed with differential N1 activation to nonscrambled vs scrambled stimuli vs both picture arrangement (n=24, $r=-0.48$, $P=.02$) and Perceptual Organization Index ($r=-0.41$, $P=.048$) scores, but not with Processing Speed Index ($r=-0.11$, $P=.61$), WMI ($r=-0.24$, $P=.29$), or BVMT-R ($r=-0.24$, $P=.29$) scores. Reduced N_{CL} generation correlated significantly with higher scores on Positive and Negative Syndrome Scale total (n=24, $r=0.46$, $P=.03$), positive ($r=0.44$, $P=.03$), and general ($r=0.45$, $P=.03$) symptoms.

COMMENT

We have previously demonstrated reduced perceptual closure ability in schizophrenia using both behavioral[11] and ERP[11] measures, along with impaired generation of the dorsal stream P1 potential,[35] suggesting significant con-

Table 3. Neuropsychological Test Scores and Their Probability Levels Relative to Normative Means for Schizophrenic Patients

Measure	Score, Mean (SD)	*P* Value	Normative Mean	Ventral Stream (LOC)		Hippocampus	
				r	*P* Value	*r*	*P* Value
Picture arrangement	8.4[a] (3.7)	.03	10	0.73[a]	.01	0.65[a]	.03
Perceptual Organization Index	89.1[a] (16.9)	.003	100	0.67[a]	.02	0.6	.052
Picture completion	7.1[a] (3.1)	.001	10	0.5	.12	0.75[a]	.008
Matrix reasoning	9.2 (3.4)	.22	10	0.74[a]	.009	0.62[a]	.04
Block design	8.3[a] (3.2)	.01	10	0.41	.21	0.39	.23
Processing Speed Index	80.5[a] (8.6)	.001	100	0.3	.4	0.3	.4
Working Memory Index	88.2[a] (14.7)	.001	100	−0.16	.65	0.25	.46
Brief Visual Memory Test	16.3[a] (8.6)	.001	25	0.35	.28	0.67[a]	.02

Abbreviation: LOC, lateral occipital complex.
[a] $P < .05$.

tribution of early visual impairments[36] to more complex forms of visual processing. Since that time, additional evidence has accumulated regarding the functional anatomy of the perceptual closure process using scalp ERP, fMRI, and direct intracranial recordings in humans, permitting more detailed hypothesis-driven analysis of underlying physiological disturbances in schizophrenia.

This study confirms and extends previous findings in 4 ways. First, it replicates the prior reports of impaired P1 and N_{CL} generation using a more efficient paradigm we recently used in healthy individuals.[3,10] Second, it combines ERP findings with results of parallel fMRI investigation, permitting an improved characterization of the deficit in schizophrenia, while third, providing a direct between-group comparison of fMRI activation patterns in patients and controls. Finally, neuropsychological data were collected to enable the characterization of the functional neuroanatomy of closure processes more fully within the context of neuropsychological dysfunction in schizophrenia.

Here, as in previous studies, the earliest deficits were found in generation of the dorsal stream P1 potential, suggesting failure of magnocellular and/or early-stage cortical processing, followed by impaired generation of N_{CL}.[17,37,38] Although cortical visual area V1 activation was not assessed in this study relative to fragmented images, patients participating in this study were previously found to have reduced activation to magnocellular-biased visual stimuli.[36]

In addition, in the present study, specific measures were obtained for other brain regions that have been found to be involved in the closure process, including the PFC and hippocampus.[3] Deficits in dorsal activation significantly predicted deficits in frontal processing as assessed using both ERP and fMRI measures. In both the ERP and fMRI experiments, the degree of correlation between dorsal and prefrontal activation was similar in patients and controls, suggesting relatively normal functional connectivity between these 2 regions in patients. However, the absolute level of activation was dramatically reduced over both brain regions in patients, suggesting that failure in processing at the level of dorsal stream visual cortex contributes directly to failures in processing at subsequent nodes in the closure network.

The study also permits the first assessment of potential hippocampal involvement in perceptual closure deficits in schizophrenia. Although the hippocampus does not generate known scalp-recordable activity because of its location and orientation within the brain, we have recently demonstrated the involvement of hippocampal formation in the process of closure using recordings from intracranial electrodes in epileptic patients.[3] In those recordings, a significant sustained β-synchrony interaction was observed between the hippocampal formation and LOC during the N_{CL} time frame, suggesting that closure may depend on a matching process between sensory inputs and mnemonic representations activated within the hippocampus.

In support, Bar and coworkers[39,40] have postulated that the magnocellular system provides rapid low-resolution input to the frontal cortex, which then helps trigger top-down object recognition. The failure of frontal and hippocampal activation observed here would be consistent with the hypothesis that this top-down mechanism is lost in schizophrenia, owing at least in part to loss of ascending magnocellular/dorsal stream input. However, intrinsic abnormalities in prefrontal and hippocampal function and structure have also been reported,[41] leaving the degree to which intrinsic prefrontal and hippocampal pathology and deficit in top-down processes may contribute to perceptual closure ability unresolved as well.

As in our earlier studies, prominent closure-related activity was observed in nonscrambled vs scrambled objects in the LOC, consistent with the concept that LOC represents the locus of conscious object identification.[39,42] However, several lines of evidence suggest that activation deficits were not due to intrinsic structural dysfunction within the LOC.

First, generation of the N1 potential, which reflects initial activation of the LOC primarily via the parvocellular stream, was unimpaired. Second, we have previously demonstrated intact N1 modulation in schizophrenia by illusory contour stimuli.[9] As opposed to perceptual closure, which depends on recursive processing between brain regions and thus occurs significantly after the visual N1, illusory contour-related activity overlaps the N1, suggesting that it can be processed during the feed-forward sweep.[13] Behavioral modulations of perceptual closure, such as repetition and word priming are also relatively intact,[43] suggesting intact intrinsic function of the LOC and modulation by top-down influences.

Third, in our path analysis, illness-related effects were observed only at the level of the dorsal stream visual cortex, and, to a lesser extent, PFC, suggesting that impaired activation of the LOC in this task was driven primarily by impaired input from preceding stages of cortical analysis. Other studies have also demonstrated intact ventral stream function to stimuli like faces using behavioral[44] and fMRI[45] measures.

Finally, this study assesses closure-related activity relative to traditional neuropsychological measures. Performance IQ in the WAIS is made up of 2 indices: the Perceptual Organization Index and Processing Speed Index. Reduced performance IQ is a hallmark of schizophrenia. In the present sample, significant reductions in both the Perceptual Organization Index and Processing Speed Index were observed relative to normative values, though reductions in the Processing Speed Index were significantly more robust ($P = .003$), consistent with prior publications.[46] Nevertheless, herein, impaired activation of the LOC correlated specifically with overall Perceptual Organization Index impairment, as well as reduced picture arrangement scores, but not with impairments in Processing Speed Index, WMI, or BVMT-R scores (Table 3). Thus as expected, LOC impairment was most related to cognitive difficulties in perceptual organization.

A significant correlation was also observed between hippocampal activation and picture arrangement scores, and a nearly significant correlation with Perceptual Organization Index was also observed (Table 3), suggesting that the interaction between the hippocampus and LOC may also be critical for successful completion of these tasks. In terms of subtests, a somewhat different pattern of correlations was observed between regions, with LOC activation correlating only with matrix reasoning, and hippocampal activation correlating with both picture completion and matrix reasoning. The differential pattern of correlation may reflect the different mnemonic requirements of the picture completion vs matrix reasoning subtests, as hippocampal activation correlated also with performance on the BVMT-R, whereas the LOC did not. As with the LOC, hippocampal activity in this task did not correlate significantly with performance on either the Processing Speed Index or WMI, suggesting relative independence of perceptual closure mechanisms from other aspects of cognitive dysfunction.

The study is potentially limited by the small sample size, which suggests that replication in a larger group of subjects may be warranted, and by the relatively high doses of antipsychotic medication. However, no correlation was observed between any of the dependent measures and chlorpromazine equivalents, which argues against direct medication effects. Additionally, a more balanced sex distribution would have been preferable. However, 2 previous studies of closure[10,43] with a more balanced population indicated no sex differences in the performance of this task.

In summary, the present study represents the first multimodal imaging study of impaired perceptual closure ability in schizophrenia and highlights the importance of distributed network dysfunction in the pathophysiology of cognitive dysfunction. In the case of perceptual closure, the critical network of regions begins in the dorsal stream visual cortex and encompasses the PFC, hippocampus, and ventral stream visual regions as well. Deficits in early stages of processing contribute significantly to impairments in subsequent frontal, hippocampal, and ventral stream processing. Dysfunction within this network also contributes to overall performance IQ impairments in schizophrenia, with particular relevance to functions relating to processing of complex visual scenes. Overall, sensory input dysfunction must be considered a strong contributor to neurocognitive dysfunction in schizophrenia.

Submitted for Publication: June 10, 2009; final revision received October 26, 2009; accepted November 16, 2009.
Author Affiliations: Conte Center for Schizophrenia Research, Cognitive Neurophysiology Laboratory, Nathan S. Kline Institute for Psychiatric Research, Orangeburg, New York (Drs Sehatpour, Dias, Butler, Revheim, Guilfoyle, Foxe, and Javitt); Departments of Psychiatry and Neuroscience, New York University Langone School of Medicine, New York, New York (Drs Sehatpour, Butler, and Javitt); and Program in Cognitive Neuroscience, Department of Psychology, The City College of the City University of New York North Academic Complex, New York (Drs Sehatpour, Butler, Foxe, and Javitt).
Correspondence: Pejman Sehatpour, MD, PhD, Nathan S. Kline Institute for Psychiatric Research, Schizophrenia Research Center, 140 Old Orangeburg Rd, Orangeburg, NY 10962 (sehatpour@nki.rfmh.org).
Financial Disclosure: None reported.
Funding/Support: This work was supported by grants MH49334 and MH84848 from the National Institute of Mental Health (Dr Javitt) and grant P50MH086385 from the New York University Conte Center for Schizophrenia Research.
Additional Contributions: We are ever grateful to all participants, particularly the patients who donated their time and energy with grace and dignity to this project. Maria Jalbrzikowski, MA, assisted in data collection and analysis and Talia Kaplan, BA, and Heather Glubo, MA, aided in manuscript preparation.

REFERENCES

1. Green MF, Kern RS, Braff DL, Mintz J. Neurocognitive deficits and functional outcome in schizophrenia: are we measuring the "right stuff"? *Schizophr Bull.* 2000; 26(1):119-136.
2. Nuechterlein KH, Green MF, Kern RS, Baade LE, Barch DM, Cohen JD, Essock S, Fenton WS, Frese FJ 3rd, Gold JM, Goldberg T, Heaton RK, Keefe RS, Kraemer H, Mesholam-Gately R, Seidman LJ, Stover E, Weinberger DR, Young AS, Zalcman S, Marder SR. The MATRICS Consensus Cognitive Battery, part 1: test selection, reliability, and validity. *Am J Psychiatry.* 2008;165(2):203-213.
3. Sehatpour P, Molholm S, Schwartz TH, Mahoney JR, Mehta AD, Javitt DC, Stanton PK, Foxe JJ. A human intracranial study of long-range oscillatory coherence across a frontal-occipital-hippocampal brain network during visual object processing. *Proc Natl Acad Sci U S A.* 2008;105(11):4399-4404.
4. Malach R, Reppas JB, Benson RR, Kwong KK, Jiang H, Kennedy WA, Ledden PJ, Brady TJ, Rosen BR, Tootell RB. Object-related activity revealed by functional magnetic resonance imaging in human occipital cortex. *Proc Natl Acad Sci U S A.* 1995;92(18):8135-8139.
5. Doniger GM, Foxe JJ, Murray MM, Higgins BA, Snodgrass JG, Schroeder CE, Javitt DC. Activation time course of ventral visual stream object-recognition areas: high density electrical mapping of perceptual closure processes. *J Cogn Neurosci.* 2000;12(4):615-621.

6. Schroeder CE, Mehta AD, Givre SJ. A spatiotemporal profile of visual system activation revealed by current source density analysis in the awake macaque. *Cereb Cortex*. 1998;8(7):575-592.
7. Varela F, Lachaux JP, Rodriguez E, Martinerie J. The brainweb: phase synchronization and large-scale integration. *Nat Rev Neurosci*. 2001;2(4):229-239.
8. Murray MM, Foxe DM, Javitt DC, Foxe JJ. Setting boundaries: brain dynamics of modal and amodal illusory shape completion in humans. *J Neurosci*. 2004; 24(31):6898-6903.
9. Foxe JJ, Murray MM, Javitt DC. Filling-in in schizophrenia: a high-density electrical mapping and source-analysis investigation of illusory contour processing. *Cereb Cortex*. 2005;15(12):1914-1927.
10. Sehatpour P, Molholm S, Javitt DC, Foxe JJ. Spatiotemporal dynamics of human object recognition processing: an integrated high-density electrical mapping and functional imaging study of "closure" processes. *Neuroimage*. 2006; 29(2):605-618.
11. Doniger GM, Foxe JJ, Murray MM, Higgins BA, Javitt DC. Impaired visual object recognition and dorsal/ventral stream interaction in schizophrenia. *Arch Gen Psychiatry*. 2002;59(11):1011-1020.
12. Bar M, Kassam KS, Ghuman AS, Boshyan J, Schmid AM, Schmidt AM, Dale AM, Hämäläinen MS, Marinkovic K, Schacter DL, Rosen BR, Halgren E. Top-down facilitation of visual recognition. *Proc Natl Acad Sci U S A*. 2006;103(2):449-454.
13. Lamme VAF, Roelfsema PR. The distinct modes of vision offered by feedforward and recurrent processing. *Trends Neurosci*. 2000;23(11):571-579.
14. Miyashita Y, Hayashi T. Neural representation of visual objects: encoding and top-down activation. *Curr Opin Neurobiol*. 2000;10(2):187-194.
15. Marr D, Nishihara HK. Representation and recognition of the spatial organization of three-dimensional shapes. *Proc R Soc Lond B Biol Sci*. 1978;200(1140): 269-294.
16. Bussey TJ, Saksida LM, Murray EA. Perirhinal cortex resolves feature ambiguity in complex visual discriminations. *Eur J Neurosci*. 2002;15(2):365-374.
17. Butler PD, Schechter I, Zemon V, Schwartz SG, Greenstein VC, Gordon J, Schroeder CE, Javitt DC. Dysfunction of early-stage visual processing in schizophrenia. *Am J Psychiatry*. 2001;158(7):1126-1133.
18. Wechsler D. *The Wechsler Adult Intelligence Scale*. 3rd ed. San Antonio, TX: The Psychological Corporation; 1997.
19. First MB, Spitzer RL, Gibbon M, Williams J. *Structural Clinical Interview for DSM-IV Axis I Disorders (SCID-IV)*. New York, NY: Biometrics Research Department, New York State Psychiatric Institute; 1997.
20. Overall JE, Gorham DR. The Brief Psychiatric Rating Scale. *Psychol Rep*. 1962; 10:799-812.
21. Andreasen NC. *The Scale for the Assessment of Negative Symptoms (SANS)*. Iowa City, IA: The University of Iowa; 1984.
22. Snodgrass JG, Vanderwart M. A standardized set of 260 pictures: norms for name agreement, image agreement, familiarity, and visual complexity. *J Exp Psychol Hum Learn*. 1980;6(2):174-215.
23. Cycowicz YM, Friedman D, Rothstein M, Snodgrass JG. Picture naming by young children: norms for name agreement, familiarity, and visual complexity. *J Exp Child Psychol*. 1997;65(2):171-237.
24. Snodgrass JG, Corwin J. Perceptual identification thresholds for 150 fragmented pictures from the Snodgrass and Vanderwart picture set. *Percept Mot Skills*. 1988;67(1):3-36.
25. Goebel R, Linden DE, Lanfermann H, Zanella FE, Singer W. Functional imaging of mirror and inverse reading reveals separate coactivated networks for oculomotion and spatial transformations. *Neuroreport*. 1998;9(4):713-719.
26. Talairach J, Tournoux P. *Co-Planar Stereotaxic Atlas of the Human Brain*. New York, NY: Thieme; 1988.
27. Boynton GM, Engel SA, Glover GH, Heeger DJ. Linear systems analysis of functional magnetic resonance imaging in human V1. *J Neurosci*. 1996;16(13): 4207-4221.
28. Benjamini Y, Hochberg Y. Controlling the false discovery rate: a practical and powerful approach to multiple testing. *J R Stat Soc Series B Stat Methodol*. 1995; 57(1):289-300.
29. Genovese CR, Lazar NA, Nichols T. Thresholding of statistical maps in functional neuroimaging using the false discovery rate. *Neuroimage*. 2002;15(4): 870-878.
30. Friston KJ, Frith CD, Frackowiak RS, Turner R. Characterizing dynamic brain responses with fMRI: a multivariate approach. *Neuroimage*. 1995;2(2):166-172.
31. Friston KJ, Frith CD, Liddle PF, Dolan RJ, Lammertsma AA, Frackowiak RS. The relationship between global and local changes in PET scans. *J Cereb Blood Flow Metab*. 1990;10(4):458-466.
32. Wechsler D. *The Wechsler Memory Scale-III*. San Antonio, TX: The Psychological Corporation; 1997.
33. Benedict RHB, Brandt J, Staff PAR. *Brief Visuospatial Memory Test-Revised*. Lutz, FL: Psychological Assessment Resources, Inc; 2007.
34. Arbuckle JL. *Amos 7.0 User's Guide. Spring House*. Chicago, IL: Amos Development Corporation; 2006.
35. Foxe JJ, Doniger GM, Javitt DC. Early visual processing deficits in schizophrenia: impaired P1 generation revealed by high-density electrical mapping. *Neuroreport*. 2001;12(17):3815-3820.
36. Martínez A, Hillyard SA, Dias EC, Hagler DJ Jr, Butler PD, Guilfoyle DN, Jalbrzikowski M, Silipo G, Javitt DC. Magnocellular pathway impairment in schizophrenia: evidence from functional magnetic resonance imaging. *J Neurosci*. 2008; 28(30):7492-7500.
37. Butler PD, Zemon V, Schechter I, Saperstein AM, Hoptman MJ, Lim KO, Revheim N, Silipo G, Javitt DC. Early-stage visual processing and cortical amplification deficits in schizophrenia. *Arch Gen Psychiatry*. 2005;62(5):495-504.
38. Butler PD, Martinez A, Foxe JJ, Kim D, Zemon V, Silipo G, Mahoney J, Shpaner M, Jalbrzikowski M, Javitt DC. Subcortical visual dysfunction in schizophrenia drives secondary cortical impairments. *Brain*. 2007;130(pt 2):417-430.
39. Bar M, Tootell RBH, Schacter DL, Greve DN, Fischl B, Mendola JD, Rosen BR, Dale AM. Cortical mechanisms specific to explicit visual object recognition. *Neuron*. 2001;29(2):529-535.
40. Kveraga K, Boshyan J, Bar M. Magnocellular projections as the trigger of top-down facilitation in recognition. *J Neurosci*. 2007;27(48):13232-13240.
41. Heckers S. Hippocampus. In: Javitt D, Kantrowitz J, eds. Handbook of Neurochemistry and Molecular Neurobiology. 3rd ed. New York, NY: Springer Science+Business LLC; 316-330.
42. Lerner Y, Hendler T, Malach R. Object-completion effects in the human lateral occipital complex. *Cereb Cortex*. 2002;12(2):163-177.
43. Doniger GM, Silipo G, Rabinowicz EF, Snodgrass JG, Javitt DC. Impaired sensory processing as a basis for object-recognition deficits in schizophrenia. *Am J Psychiatry*. 2001;158(11):1818-1826.
44. Butler PD, Tambini A, Yovel G, Jalbrzikowski M, Ziwich R, Silipo G, Kanwisher N, Javitt DC. What's in a face? effects of stimulus duration and inversion on face processing in schizophrenia. *Schizophr Res*. 2008;103(1-3):283-292.
45. Yoon JH, D'Esposito M, Carter CS. Preserved function of the fusiform face area in schizophrenia as revealed by fMRI. *Psychiatry Res*. 2006;148(2-3):205-216.
46. Wilk CM, Gold JM, McMahon RP, Humber K, Iannone VN, Buchanan RW. No, it is not possible to be schizophrenic yet neuropsychologically normal. *Neuropsychology*. 2005;19(6):778-786.